The International Journal Of Engineering And Science (IJES)
||Volume||2 ||Issue|| 8 ||Pages|| 08-17||2013||
ISSN(e): 2319 – 1813 ISSN(p): 2319 – 1805

Comparative Analysis of K-ε and Spalart-Allmaras Turbulence Models for Compressible Flow through a Convergent-Divergent Nozzle

Nadeem Akbar Najar[#1], D Dandotiya[1], Farooq Ahmad Najar[2]
[1]*Department of Mechanical Engineering*
SRCEM Gwalior C/O Rajiv Gandhi Technological University
Bhopal MP, India
[2]*Department of Mechanical Engineering*
National Institute of Technology
Hazratbal Srinagar

----------ABSTRACT----------

Owing to its peculiar flow characteristics, a convergent-divergent nozzle finds its application in various aerospace technologies and non aerospace technologies as well. Therefore, it is necessary to understand flow fields associated with these nozzles to explore their capabilities to their fullest. In this paper, 2D, axisymetric flow analysis of compressible flow through a convergent-divergent nozzle is carried out with the help of CFD tools (Gambit 2.2.30 for modeling and Fluent 6.3.26 for analysis). First the problem is solved by employing K-ε turbulence model and afterwards by employing Spalart-Allmaras turbulence model, a comparative analysis is carried out between the models on the basis pressure, velocity, temperature contours and vectors to ascertain the efficient design conditions for convergent-divergent nozzles, suitability of models for a particular application and interaction between various flow field characteristics resulting in the flow separation and shock waves.

INDEX TERMS: *Convergent-divergent nozzle, axisymetric flow, K-ε turbulence model, Spalart- Allmaras model, CFD, flow separation, shock waves.*

Date of Submission: 6 , August ,2013  Date of Acceptance:25,August ,2013

I. INTRODUCTION

Computational fluid dynamics is a versatile technique of modeling and simulation of flow fields which provides accurate results regarding the flow characteristics of devices like flow over an airfoil, if simulated using CFD code provides the user with each and everything required for the efficient designing- pressure, velocity, density at each fluid element. CFD plays a vital role in modern techniques of design optimization by providing the offhand solutions of the flow problems. The solution of Reynolds averaged Navier-Stokes (RANS) equations being transient in nature imposes the complexity in the computational studies of the flow field through CD nozzles and the implementation of an appropriate turbulence model for closure of the RANS equations. Generalized coordinates and conservative form are used to solve the governing equations. The numerical studies carried out by various researchers have assessed the accuracy of the turbulence model for predicting the flow filed and the nozzle performance accurately. The compressible flow regions in nozzles being dominated by strong pressure gradients and complex secondary flows induce discrepancies between the numerical simulations and the experimental measurements. In this paper, flow through a convergent-divergent nozzle has been modeled and simulated using CFD code employing two turbulence models- K-ε turbulence model and Spalart- Allmaras turbulence model. Design of the nozzle has been carried out in Gambit 2.2.30 environment by submitting the readymade coordinates and simulation of flow using turbulence models has been carried out in Fluent 6.3.26 environment.

II. LITERATURE REVIEW:

A. A. Khan and T. R. Shembharkar [1] confirmed that the classical one-dimensional inviscid theory does not reveal the complex flow features in a choked CD nozzle accurately. They used the code Fluent to compute RANS flow in a 2-D CD nozzle for nozzle pressure ratios (NPR) corresponding to presence of shock inside the diverging part of the nozzle. The computed solutions differed from the simple theory so far as shock location, shock structure and after-shocks are concerned. Nathan Spotts et al [3] performed a CFD study of the compressible flow through convergent-conical nozzles to investigate the effect of the nozzle pressure ratio and nozzle angle on the nozzle performance and confirmed that the discharge coefficient increases as the nozzle angle decreases and the choked nozzle pressure ratio is lower for a smaller nozzle angle. The discharge coefficient increases with increasing pressure ratio until the choked condition is reached. The thrust coefficient

increases as the nozzle angle increases, and for a given nozzle angle, the thrust coefficient decreases as nozzle pressure ratio increases.

P. Padmanathan and Dr. S. Vaidyanathan [4] carried out the computational investigation for different nozzle NPR values. Shock structure is formed near the exit of the nozzle by varying the exit pressure. The considered NPR values are 1.63, 1.59, 1.55 and 1.52. They observed that for NPR below 1.52 there is no formation of shock and for NPR above 1.63 reversible flows is detected and the computational solution tends to be more precise.

Pardhasaradhi Natta et al [5] found in the nozzles with different divergence angles considering default divergence angle as 7 degrees that; In the nozzle with divergence angle of 20 degrees Mach number is 1.15 at throat and at divergence angle of 7 degrees Mach number is 1.19. From Default angle Mach number is increasing up to 2.917 at the nozzle exit while for divergence angle of 20 degrees the Mach number at exit is nearly 2.84. At the throat the velocity magnitude is same for all divergence degrees of angle and it is 260 m/s.. Near the wall, the Mach number is decreasing for all the nozzles. This is due to the viscosity and turbulence in the fluid. For a nozzle of divergence angle of 20 degrees the Mach number at exit is very low compared to other nozzles. While when the divergence angle is 30 degrees the Mach number at nozzle exit is 3.06 and but an divergence angle 40 degrees it gives the Mach number at nozzle exit is 3.19 and it is lowest at an divergence angle 20 degrees. The turbulence intensity is very high for a divergence angle of 20 degrees at exit. For maximum velocity we can go with 30 or 40 degrees of divergence angle conical nozzle.
The efficiency of the nozzle increases as we increase the divergence angle of the nozzle up to certain extent.

Nozzle Governing Equations: For the flow analysis of nozzles, mass, momentum and energy need to be conserved that is, the following laws should be obeyed by the field under observation;
Law of Conservation of Mass- Continuity Equation [2]
Law of Conservation of Momentum- Momentum Equation [2]
Law of Conservation of Energy- Energy Equation [2]

Continuity Equations
Non Conservation Form
$$D\rho / Dt + \rho \nabla . V = 0 \quad \text{Eq.1}$$
Conservation Form
$$\partial p/\partial t + \nabla .(\rho V)=0 \quad \text{Eq.2}$$
Momentum Equations
Non Conservation Form
$$\rho\, Du / Dt = -\partial p/\partial x + \rho f_x \quad \text{(X –Component)} \quad \text{Eq. 3}$$
$$\rho\, Dv/ Dt = -\partial p/ \partial y + \rho f_y \quad \text{(Y- Component)} \quad \text{Eq. 4}$$
$$\rho\, Dw/ Dt = -\partial p/\partial z + \rho f_z \quad \text{(Z- Component)} \quad \text{Eq. 5}$$

Conservation Form
$$\partial (\rho u)/ \partial t + \nabla .(\rho uV) = -\partial p/\partial x + \rho f_x \text{ ----- (X-Component)} \quad \text{Eq. 6}$$
$$(\rho v)/\partial t + \nabla . (\rho vV) = -\partial p/\partial y + \rho f \text{ ----- (Y-Component)} \quad \text{Eq. 7}$$
$$(\rho w)/\partial t + \nabla .(\rho wV)= -\partial p/\partial z + \rho f_z \text{ ----- (Z-Component)} \quad \text{Eq. 8}$$

Energy Equation

Non Conservation Form
$$\rho D/Dt(e + V^2/2) = \rho q - \partial/\partial x(up) - \partial/\partial y(vp) - \partial/\partial z(wp) + \rho f.V \quad \text{Eq. 9}$$

Conservation Form
$$\partial/\partial t [\rho(e + V^2/2)] + \nabla .[\rho(e + V^2/2) V] = \rho q - \partial /\partial x(up) - \partial/\partial y(vp) - \partial/\partial z(wp) + \rho f.V \quad \text{Eq. 10}$$

III. TURBULENCE MODELING

Turbulence Models: The mathematical models selected for this work are the standard K-ε model and Spalart-Allmaras model which are based on the Reynolds Averaged Navier-Stoke (RANS) model available in Fluent.

K-ε Model: The standard K-ε model is the most widely used transport model. The standard K-ε model is a two-equation model and the two model equations are as follows:
The model equation for the turbulent kinetic energy K is:

$\partial/\partial t(\rho k) + \partial/\partial x_i(\rho k u_i) = \partial/\partial x_j [(\mu + \mu_t/\sigma_k)\partial k/\partial x_j] + P_k + P_b - \rho\varepsilon - Y_M + S_k$

= Rate of increase of K+ Convective transport= diffusive transport + Rate of production-Rate of destruction
The model equation for the turbulent dissipation ε is:
$\partial/\partial t(\rho\varepsilon) + \partial/\partial x_i(\rho\varepsilon u_i) = \partial/\partial x_j [(\mu + \mu_t/\sigma_\varepsilon)\partial\varepsilon/\partial x_j] + C_{1\varepsilon}\varepsilon/k (P_k + C_{3\varepsilon}P_b) - C_{2\varepsilon}\rho\varepsilon^2/k + S_\epsilon$
=Rate of increase of ε+ Convective transport= diffusive transport + Rate of production-Rate of destruction
The standard values of all the model constants as fitted with benchmark experiments are [6]:
Cμ = 0.09 ; σk=1.00 ; σε=1.30 ; Cε1=1.44 ; Cε2=1.92

Spalart-Allmaras Model: Being a one equation model, the Spalart-Allmaras model solves a modeled transport equation for the kinematic eddy (turbulent) viscosity. This embodies a class of one-equation models in which it is not necessary to calculate a length scale related to the local shear layer thickness. The Spalart-Allmaras model was designed specifically for aerospace applications involving wall-bounded flows and has given good results for boundary layers subjected to adverse pressure gradients. The turbulent dynamic viscosity is computed from
$\mu_t = \rho\nu f_{v1}$

IV.GEOMETRIC MODELING

Geometric Modeling Strategy: A four column based data relevant to nozzle design has been obtained from ANSYS tutorials and tailored and converted into three columns with Z-coordinate set as zero(as the problem is 2D based) according to Gambit requirements.

TABLE 1: NOZZLE COORDINATES

X	R(X)	Z
-0.5	0.333778669	0
-0.45	0.310303908	0
-0.4	0.287681033	0
-0.35	0.266127383	0
-0.3	0.24592425	0
-0.25	0.227431826	0
-0.2	0.211100165	0
-0.15	0.197466123	0
-0.1	0.187120297	0
-0.05	0.180628589	0
0	0.178412203	0
0.05	0.180628589	0
0.1	0.187120297	0
0.15	0.197466123	0
0.2	0.211100165	0
0.25	0.227431826	0
0.3	0.24592425	0
0.35	0.266127383	0
0.4	0.287681033	0
0.45	0.310303908	0
0.5	0.333778669	0
0.5	0.333778669	0
0.5	0	0
0.5	0	0
-0.5	0	0
-0.5	0	0
-0.5	0.333778669	0

The data is saved as a DAT file and is imported into Gambit as ICEM file. The coordinates automatically get dispensed into an upper half profile of the nozzle; no
sooner the Accept button is selected. Using Create Edge button, the coordinates of the nozzle are joined, four entities are formed as Inlet, Axis, Wall (comprising of 20 edges) and outlet. Using Create Face button, the edges are converted into a single face.

Meshing Strategy: For inlet and outlet faces, an interval count of 30 is selected and for axis, an interval count of 80 is selected and for the wall, an interval count of 4 is chosen corresponding to each edge of wall. Grading option is disabled for the sake of a coarse grid. A total of (30x80) 2400 cells are obtained in the meshed nozzle.

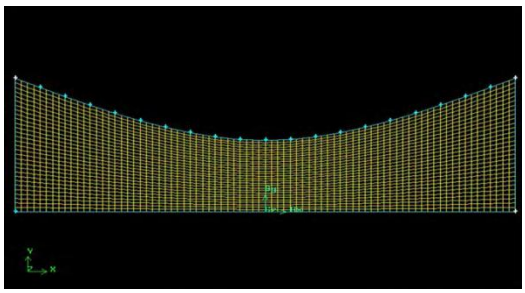

Figure 1: Meshed Profile Of 2d Nozzle

Boundary Type specification: It is very essential to specify the boundary types in the Gambit itself, to enable the Fluent understand the boundaries. Left vertical side is set as inlet against Pressure Inlet, right vertical side is assigned Pressure Outlet, bottom edge the axis and the 20 curved edges as wall, a single entity.

TABLE 2: BOUNDARY TYPES

Edge Position	Name	Type
Left	inlet	PRESSURE INLET
Right	outlet	PRESSURE OUTLET
Top	wall	WALL
Bottom	centerline	AXIS

Next, the saved mesh is exported as 2D profile to Fluent for simulation purpose.

V. FLUENT SIMULATION

Fluent Analysis :T he mesh is read as a case in the fluent choosing 2ddp, in order to arrive at accurate results, the double precision parameter is chosen.

TABLE 3: PROBLEM SET UP IN FLUENT- K EPSILON MODEL

Problem Setup	**K-Epsilon**
1. Solver 2. Formulation 3. Space 4. Time Dependency 5. Velocity Formulation 6. Gradient Option 7. Porous Formulation 8. Energy Equation 9. Viscous Model 10. Viscous Heating	Pressure Based Implicit Axisymmetric Steady Absolute Green-Gauss Cell Based Superficial Velocity ON STD K-Epsilon ON
Material Selection Air	Properties Density- Ideal Gas Cp=1006.43 Thermal Conductivity=0.0242 Viscosity=1.7894e-05 Molecular Weight=28.966
Operating Pressure	0 Pascal
Solution Controls	
Equations	Flow Modified Turbulent Viscosity Energy
Under Relaxation Factors	1. Pressure=0.3

	2. Density=1 3. Body Force=1 4. Momentum=0.7 5. Modified Turbulent Viscosity=0.8 6. Turbulent Viscosity=1 7. Energy=1
Pressure-Velocity Coupling	SIMPLE
Initialization Axial velocity	182.95 m/s
Grid Adaptation Control	Max. No. of cells=20000
Discretization Scheme	Pressure- Standard Density-2nd Order Upwind Momentum-2nd Order Upwind Turbulent Kinetic Energy-2nd Order Upwind Turbulent Dissipation Rate-2nd Order Upwind Energy-2nd Order Upwind

TABLE 4: PROBLEM SET UP FLUENT- SPALART ALLMARAS MODEL

Problem Setup	**Spalart-Allmaras**
1. Solver 2. Formulation 3. Space 4. Time Dependency 5. Velocity Formulation 6. Gradient Option 7. Porous Formulation 8. Energy Equation 9. Viscous Model 10. Viscous Heating	Pressure Based Implicit Axisymmetric Steady Absolute Green-Gauss Cell Based Superficial Velocity ON Spalart-Allmaras Vorticity Based Production ON
Material Selection Air	Properties Density- Ideal Gas Cp=1006.43 Thermal Conductivity=0.0242 Viscosity=1.7894e-05 Molecular Weight=28.966
Operating Pressure	0 Pascal
Solution Controls	
Equations	Flow Modified Turbulent Viscosity Energy
Under Relaxation Factors	1. Pressure=0.3 2. Density=1 3. Body Force=1 4. Momentum=0.7 5. Modified Turbulent Viscosity=0.8 6. Turbulent Viscosity=1 7. Energy=1
Pressure-Velocity Coupling	SIMPLE

Initialization Axial velocity	182.95 m/s
Grid Adaptation Control	Max. No. of cells=20000
Discretization Scheme	Pressure- Standard Density-2nd Order Upwind Momentum-2nd Order Upwind Modified Turbulent Viscosity-2nd Order Upwind Energy-2nd Order Upwind

VI. RESULTS AND DISCUSSIONS

A. Plots

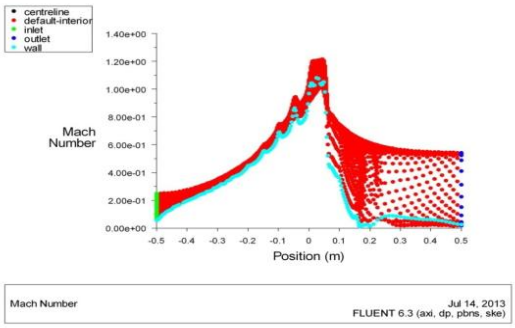

Figure 2: Mach No. Plots K-Epsilon Model

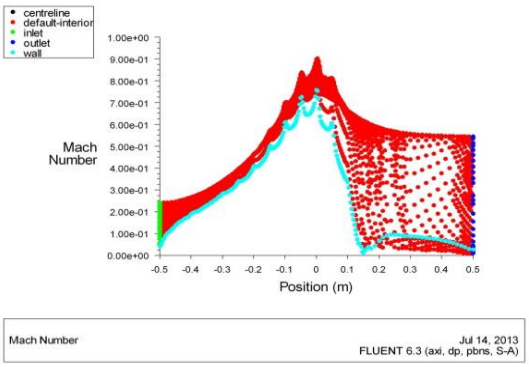

Figure 3: Mach No. Plot Spalart-Allmaras Model

The figure 3 and 4 shows the variation of Mach number across the nozzle for both models, the K-ε model indicates that the flow is subsonic at inlet and becomes supersonic at throat, after which there is a sharp decline in Mach no. indicating the shock formation immediately downstream of the throat. The Spalart- Allmaras model shows that, the flow is sub sonic at the inlet of the nozzle and becomes 0.92 Mach at throat, after the throat there is a sharp decrease in Mach number which clearly depicts the participation of compressibility effects resulting in the shocks. The K-Epsilon model shows the sharp decrease of Mach number downstream of throat whereas the Spalart-Allmaras model shows the peak Mach number (0.92) at the zero position that is exactly at the throat.

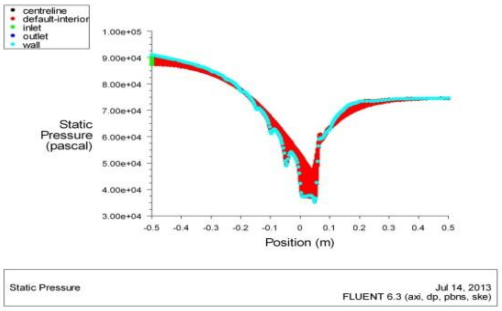

Figure 4: Static Pressure Plot K-Epsilon Model

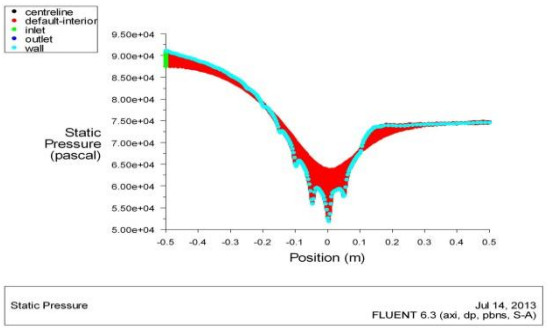

Figure 5: Satic Pressure Plot Spalart-Allmaras Model

The variation of static pressure across the nozzle is shown in figure 5 and 6, the K-Epsilon model shows the lowest point of the pressure plot downstream of the throat corresponding to supersonic velocity ,whereas the nadir lies exactly at the throat of the nozzle in case of the Spalart Allmaras model.

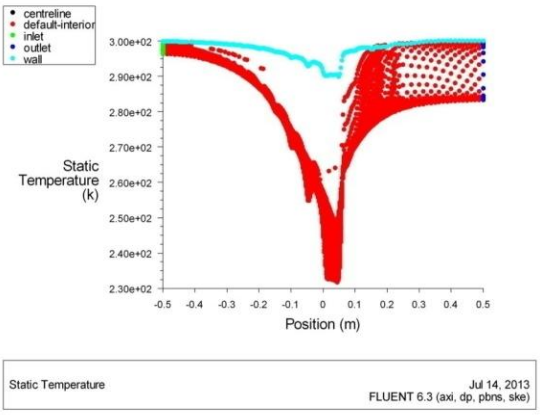

Figure 6: Static Temperature Plot K-Epsilon Model

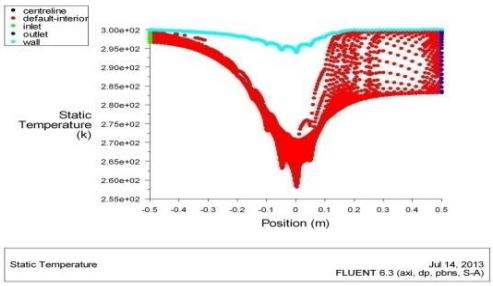

Figure 7: Static Temperature Plot Spalart-Allmaras Model

The temperature plots for both the models shown in figure 7 and 8, owing to low pressure downstream of throat the temperature also decreases from inlet to downstream of nozzle for K-Epsilon model and from inlet to zero position that is exactly throat of nozzle for Spalart-Allmaras model.

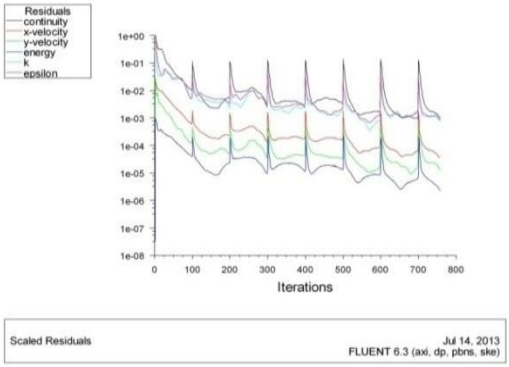

Figure 8: Residuals (Convergence) K-Epsilon Model

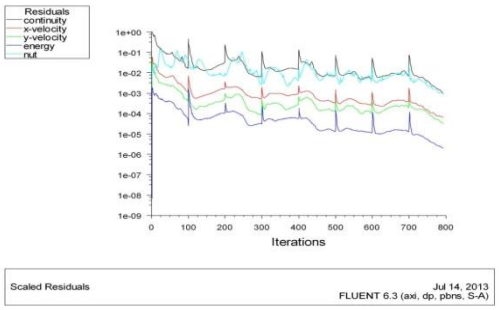

Figure 9: Residuals Spalart-Allmaras Model

Figure 9 and 10 show the convergence of solutions for both the cases, since both the cases where subjected to same set of conditions except the conditions peculiar to particular model. The convergence criteria was set to 0.001 for both cases and the solutions converged around 800 iterations both.

B. Contours

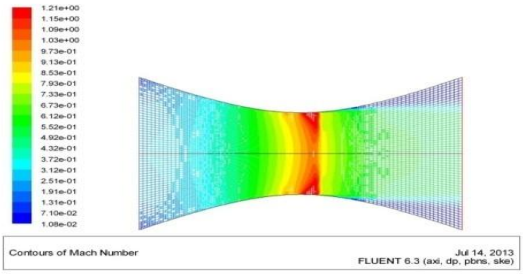

Figure 10: Mach contour k-epsilon model

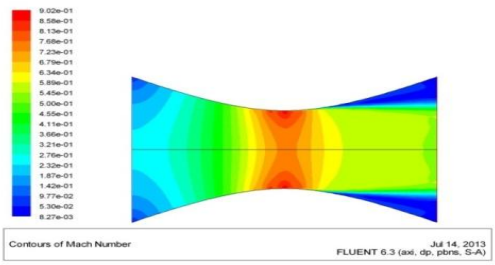

Figure 11: Mach contour spalart-allmaras model

Figure 11 and 12 show the Mach number contours for the nozzle for both the models, it can be observed in the figures that the Mach number is supersonic for a smaller length at the throat in K-Epsilon model and is subsonic throughout the nozzle for Spalart-Allmaras model. It is also observed at the walls near outlet that the Mach number is very low because of adverse pressure gradients following shock forming vortex, subjecting the flow to separation at the walls which can be clearly understood from the figure 9 showing a magnified view of velocity vectors at the exit of the nozzle. The interaction between vortex and pressure outlet results in flow reversal.

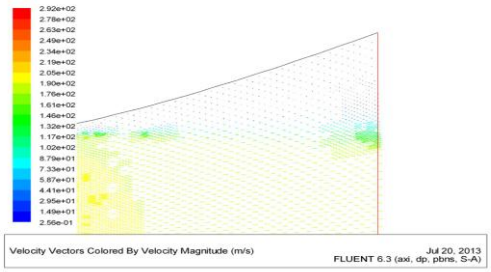

Figure 12:Magnified Velocity Vector

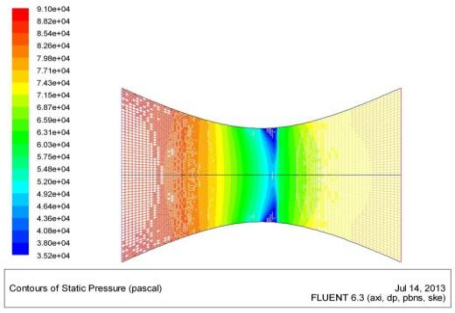

Figure 14: Pressure Contour K-Epsilon Model

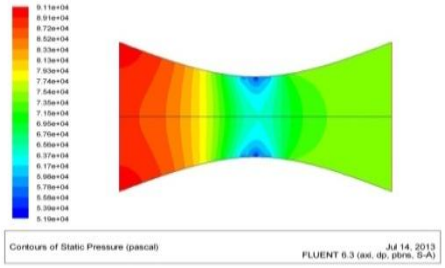

Figure 13: Pressure Contour Spalart-Allmaras Model

Figure 14 and 15, show the static pressure contours for both the models, the K-Epsilon model shows a very low pressure at the throat section indicating the presence of a shock and the Spalart-Allmaras model shows that the pressure is very low at the wall section of throat and has a diminishing effect towards centerline.

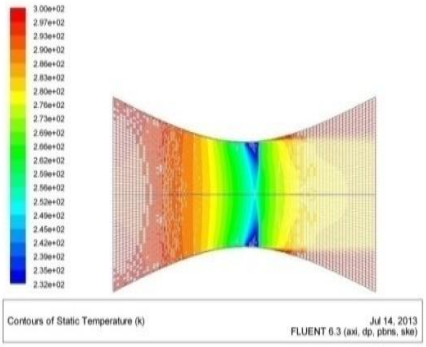

Figure 14: Temperature Contour K-Epsilon Model

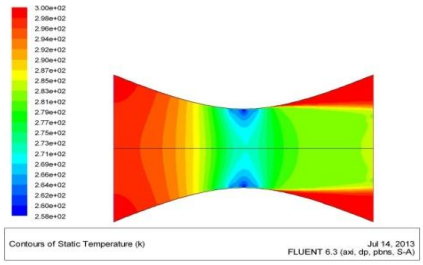

Figure 15: Temperature Contour Spalart Allmaras Model

Figures 16 and 17 show the temperature contours for both the models, owing to low pressure at throat, the temperature at throat is very low for both the models. Both the models show a very high temperature near exit walls because of flow separation due to adverse pressure gradients near the exit walls.

VII. VALIDATION

The validation of the nozzle under consideration is carried out at an inlet pressure of 101325 pa, outlet pressure of 3738.9 pa, temperature 300 K using inviscid model by comparing Mach No. plot with that of the Quasi 1 D results. It is found that results are in good agreement with each other. Figure 18, shows the scatter diagram of Mach Nos. of both the cases.

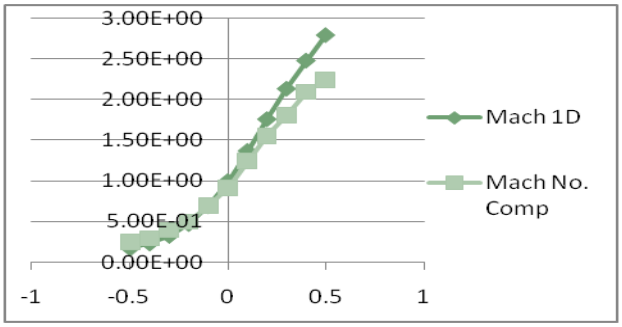

Figure 16: Nozzle Validation

VIII. CONCLUSION:

Based on the results- plots, contours and vectors obtained from the Fluent simulations, following can be concluded:

- A sharp velocity drop is obtained across the shock.
- Flow separation and formation of a vortex after the shock can be attributed to adverse pressure gradient following shocks. Reversal of flow near exit walls is due to the interaction between pressure outlet and vortex.
- The STD K- ε model turbulence model provided the accurate results as compared to Spalart-Allmaras model at same set of conditions and discretization schemes.

REFERENCES

[1] A. A. Khan and T. R. Shembharkar"Viscous Flow Analysis In A Convergent-Divergent Nozzle" Proceedings of the International Conference on Aerospace Science and Technology 26 - 28 June 2008, Bangalore, India

[2] Anderson, J.D. 1995. "Computational Fluid Dynamics", McGraw-Hill Science/Engineering/Math; 1st edition, p. 574, ISBN-0070016852 / 9780070016859.

[3] Nathan Spotts et al "A CFD analysis of compressible flow through convergent-conical nozzles" 1st AIAA Propulsion Aerodynamics Workshop , Atlanta Georgia, July 29, 2012

[4] P. Padmanathan, Dr. S. Vaidyanathan "Computational Analysis of Shockwave in Convergent Divergent Nozzle" International Journal of Engineering Research and Applications (IJERA) ISSN: 2248-9622 Vol. 2, Issue 2,Mar-Apr 2012, pp.1597-1605

[5] Pardhasaradhi Natta, V.Ranjith Kumar, Dr.Y.V.Hanumantha Rao "Flow Analysis of Rocket Nozzle Using Computational Fluid Dynamics (Cfd)" International Journal of Engineering Research and Applications (IJERA) ISSN: 2248-9622 Vol. 2, Issue 5, September- October 2012, pp.1226-1235 1226

[6] Launder and Sharma, "Applications of Energy Dissipation model of Turbulence to the calculation of flow near a spinning disc" Letters in Heat and mass transport, 1974, Pg. 131-138